Finite Element Analysis of Structures with Extruded Aluminum Profiles Having Complex Cross Sections

Abstract

Extruded aluminum profiles are widely used in building and automation structures due to their durability, lightweight, corrosion resistance, shorter fastening time and reusability. Proper design is crucial in maintaining the lifespan of these structures. It is therefore essential to determine the structural behaviors of the structures such as the natural frequency, mode shape, etc. The finite element analysis is a method which has been commonly used in determining structural behaviors. However, there are also numerous problems in analyzing these kinds of profiles using solid finite elements, such as modeling, meshing, solution time problems, etc. Therefore, beam finite elements have been used in the present study in modeling of the profiles. Furthermore, an equivalent beam element model has been developed for bolt-together connectors of the profiles. Simulation and experimental modal analysis have been conducted on example test systems. It has been demonstrated that this modeling technique is very practical and the results obtained from the method agree well with the experimental results.

Keywords

Aluminum profile, aluminum structural framing, structures, finite element analysis, ANSYS.

Serkan Güler [a]
Hira Karagülle [b]

[a] Department of Mechanical Engineering, Faculty of Mechanics, İskenderun Technical University, 31200, Hatay, Turkey,dr.serkan.guler@outlook.com

[b] Department of Mechanical Engineering, Engineering Faculty, Dokuz Eylül University, 35397, İzmir, Turkey,hira.karagulle@deu.edu.tr

1 INTRODUCTION

Modern engineering theories based on advanced engineering mathematics have been developed after the invention of the laws of motion. One of the major areas of modern engineering is the vibration theory. There are numerous studies in the literature on the vibration analysis of simple structures based on partial differential equations (Rao (2011)). The finite element (FE) method has been de-

veloped for modeling of realistic complex engineering systems. This method requires meshing of complex structures to finite elements and constructing mathematical models consisting of a set of differential equations with a large number of degrees of freedom. It has been possible to solve these equations after the development of digital computers. In the past, the analyzers constructed these equations and solved them by writing computer codes themselves. Further developments on computer softwares have made it possible to construct and solve the equations automatically. These user-friendly programs have pre-processors, solvers and post-processors (ANSYS (2009)). The users define the system under the study and make assumptions such as the types of finite elements, mesh sizes, etc. using the pre-processor. Then, they select the solution method and obtain the solutions. Finally, they evaluate the results using the post-processor. In recent years, one of the main research areas in engineering has been to develop realistic system models using these computer programs by appropriate assumptions (Akdağ et al. (2012), Zaeh et al. (2007), Wu (2004), Zaeh et al. (2004)). The accuracy of these assumptions could in turn be validated by comparing simulation results with experimental results.

Before the information age, simple structures were analyzed quantitatively and experience was very important for the analysis of complex structures. However, today, once the assumptions for the simulations are verified by experiments, complex structures can be analyzed quantitatively using validated simulation models. Thus, the importance of experience has lessened. This has enabled the researchers to develop solutions for complex engineering problems very rapidly.

Aluminum structural framing systems are widely used in industry. Aluminum profiles which have complex cross sections are preferred because they are durable, lightweight, corrosion resistant, reusable and readily available. These profiles are used in automation systems, conveyor frames, automobile body, work tables, interior design, and construction. Fewer tools and assembly time are required for assembling the system. The design is simple, and no welding and painting is required (Mazzolani (1995), Kwon et al. (2001), Mazzolani (2006)).

There are many studies which have investigated the structures that contain structural elements having simple cross sections such as square section, circular section, and rectangular section etc. (Wu (2006), Wu (2008), Hana et al. (2008), Sangle et al. (2012), Fadden et al. (2014)). On the other hand, although the aluminum structural framing systems are extensively used in industrial applications, there are limited investigations conducted for these profiles systems and their connection parts (Fiorino et al. (2013), Güler (2013), Macillo et al. (2013), Fiorino et al. (2014)). This is the motivation for the conduction of the current study.

The present study is an approach to analyze the structures of aluminum profiles having complex cross sections by using FE programs. A database has also been created for the system. The VisualBASIC (MSDN (2012)) program developed in the present study uses this database to transfer the information of the system to the pre-processor of the FE-program. ANSYS is used as the FE-program. The same database is used to obtain solid models in SolidWorks (SOLIDWORKS (2012)) by VisualBASIC commands with Application Programming Interface (API) capabilities of Solid-Works. SolidWorks has a capability to evaluate solid models which is an essential part of the design process. Meanwhile, experimental setups were established and natural frequencies measurements were conducted. For validation, the results from the present FE model have been compared with the experimental results.

2 STRUCTURES WITH ALUMINUM PROFILES

The frame of a test system (Frame-TS-1A) is shown in Fig 1. The labels for a beam (b01) and a connector (c01) are shown in the figure. The cross sections of the aluminum profiles and the connecting parts used in the frames studied in this work are shown in Tables 1 and 2. All the parts used are available in the market.
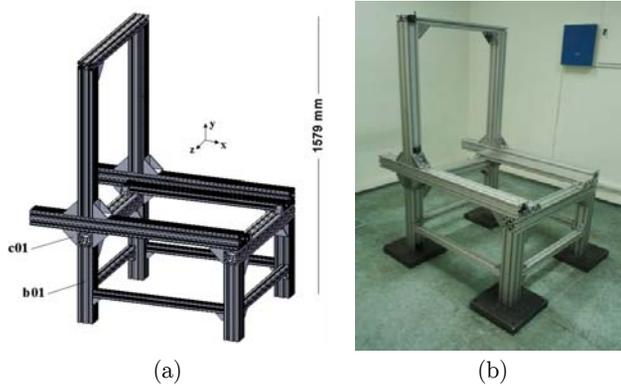

<center>(a)</center>   <center>(b)</center>

Figure 1: Solid model of frame of test system (a), photo of TS-1A (b).

Section	Size (mm)	File name	Weight (kg/m)	Area (cm^2)	Moment of inertia	
					I_x (cm^4)	I_y (cm^4)
	90x90	s90x90	10.5	39.5	302	302
	90x90	s90x90L	6.3	23.6	210	210
	45x45	s45x45L	1.5	5.7	11	11
	90x45	s90x45L	3.1	11.2	23.6	81.9
	30x30	s30x30	0.8	3.1	2.7	2.7

Table 1: Cross sections of the profiles (Bosch Rexroth AG. (2013)).

Connector	Weight(gr)	Size (mm)	File name
	314[a]+187[b]	90x90x90	cn90
	56[a]+47[b]	45x45x45	cn45
	20[a]+17[b]	30x30x30	cn30

[a]Weight of connector, [b]Weigth of bolts and nuts

Table 2: Connectors (Bosch Rexroth AG.(2013)).

Label	File name	Lb	qL
b01	s90x90	464	[0,0,400,-90,0,0]
b02	s90x90	464	[873,0,400,-90,0,0]
b03	s90x90	464	[873,0,-400,-90,0,0]
b04	s90x90	464	[0,0,-400,-90,0,0]
b05	s45x45L	783	[45,182.5,422.5,0,90,0]
b06	s45x45L	710	[895.5,182.5,-355,0,0,0]
b07	s45x45L	783	[45,182.5,-422.5,0,90,0]
b08	s45x45L	710	[-22.5,182.5,-355,0,0,0]
b09	s90x90	890	[873,509,-445,0,0,90]
b10	s90x90	890	[0,509,-445,0,0,90]
b11	s90x90L	1250	[-332,599,-400,90,0,90]
b12	s90x90L	1250	[-332,599,-400,90,0,90]
b13	s90x45L	963	[-45,576.5,310,90,0,90]
b14	s90x45L	963	[-45,576.5,-310,90,0,90]
b15	s90x90L	890	[0,644,400,-90,0,0]
b16	s90x90L	890	[0,644,-400,-90,0,0]
b17	s90x45L	890	[0,1556.5,-445,0,0,90]
c01	cn45	-	[45,160,422.5,90,90,0]
c02	cn45	-	[828,160,422.5,0,-90,90]
c03	cn45	-	[895.5,160,355,90,180,0]
c04	cn45	-	[895.5,160,-355,90,0,0]
c05	cn45	-	[828,160,-422.5,0,-90,90]
c06	cn45	-	[45,160,-422.5,90,90,0]
c07	cn45	-	[-22.5,160,-355,90,0,0]
c08	cn45	-	[-22.5,160,355,90,180,0,]
c09	cn90	-	[45,554,400,0,90,-90]
c10	cn90	-	[828,554,400,0,-90,90]
c11	cn90	-	[873,464,355,90,180,0]
c12	cn90	-	[873,464,-355,90,0,0]
c13	cn90	-	[828,554,-400,0,-90,90]
c14	cn90	-	[45,554,-400,0,90,-90]
c15	cn90	-	[0,464,-355,90,0,0]
c16	cn90	-	[0,464,355,90,180,0]
c17	cn90	-	[-45,554,400,0,-90,90]
c18	cn90	-	[-45,554,-400,0,-90,90]
c19	cn45	-	[896.5,554,265,-90,0,0]
c20	cn45	-	[896.5,554,-265,0,0,0]
c21	cn45	-	[-23.5,554,265,-90,0,0]
c22	cn45	-	[-23.5,554,-265,0,0,0]
c23	cn90	-	[0,1534,355,90,180,0]
c24	cn90	-	[0,1534,-355,90,0,0]
c25	cn90	-	[45,644,400,0,90,0]
c26	cn90	-	[-45,644,400,0,-90,0]
c27	cn90	-	[45,644,-400,0,90,0]
c28	cn90	-	[-45,644,-400,0,-90,0]
c29	cn45	-	[45,205,422.5,0,90,0]
c30	cn45	-	[828,205,422.5,0,-90,0]
c31	cn45	-	[895.5,205,355,-90,0,0]
c32	cn45	-	[895.5,205,-355,0,0,0]
c33	cn45	-	[828,205,-422.5,0,-90,0]
c34	cn45	-	[45,205,-422.5,0,90,0]
c35	cn45	-	[-22.5,205,-355,0,0,0]
c36	cn45	-	[-22.5,205,355,-90,0,0]

Table 3: Database for Frame-TS-1A

A database was created in a text file containing the information about the structure of the frame. The information about a beam is given by the label, the section file name, L_b, and $qL = [x_0, y_0, z_0, \vartheta_x, \vartheta_y, \vartheta_z]$. L_b is the length of the beam while qL is the location of the beam. x_0, y_0, and z_0 are the Cartesian coordinates of the local origin of the beam in the global coordinate system. ϑ_x, ϑ_y, ϑ_z are the rotation angles of the beam about the local x, y, and z axes, respectively. The beam is located at the origin and it is oriented in the global z axis for $qL = qL_0 = [0, 0, 0, 0, 0, 0]$. The distances are given in mm, and the angles are given in degree, unless otherwise stated.

The information about a connector is given by the label, the solid model file name, and qL. qL is the location of the connector. The labels start with the characters b and c for the beams and connectors, respectively. The database for the frame in Figure 1 is given in Table 3.

3 FINITE ELEMENT MODELS

3.1 Modeling with Solid Finite Elements

The easiest way of FE analysis after constructing solid model of the system is by using solid finite elements. ANSYS can use SolidWorks models, consider contacting surfaces, and perform meshing to generate solid finite elements. The user defines the boundary conditions and obtains the solution.

The disadvantages of this approach for complex systems are that the resulting number of elements and degrees of freedom may be too large, meshing problems may arise, solution times may be too long, high performance computers may be required solutions may not be obtained, and analysis may not be practical.

Small gaps (1 mm) between connected beams are given in the solid model as shown in Figure 2 for FE analyses. The gaps are given as decreasing lengths of beams. In this assumption, connected beam faces are mated to connector faces only and there is no direct contact between beams. The results are presented below for the models with gaps.
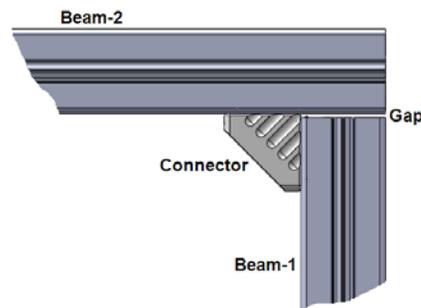

Figure 2: Gap given between connected beams

SOLID186 and SOLID187 elements are used in ANSYS. They are 3-dimensional 20-node and 10-node structural finite elements, respectively. Each node has three degrees of freedom (nodal translations in x, y, and z directions). The material properties of finite elements are defined by $p_m = [E, \rho, \upsilon, \beta]$. E is the modulus of elasticity (GPa), ρ is the density (kg/m^3), υ is the Poisson's ratio,

and β is the stiffness matrix multiplier for damping. Material properties are p_m=[69,2700,0.3,0] for aluminum in this study.

3.2 Modeling with Beam Elements

Due to the disadvantages of the solid FE modeling as described above, the beam finite elements are used. In this approach, firstly, the lines are assigned for beams. The section attributes are defined for the lines. Two beams with a connector are shown in Figure 3 (a). The lines for the beam FE model are shown in Figure 3 (b).
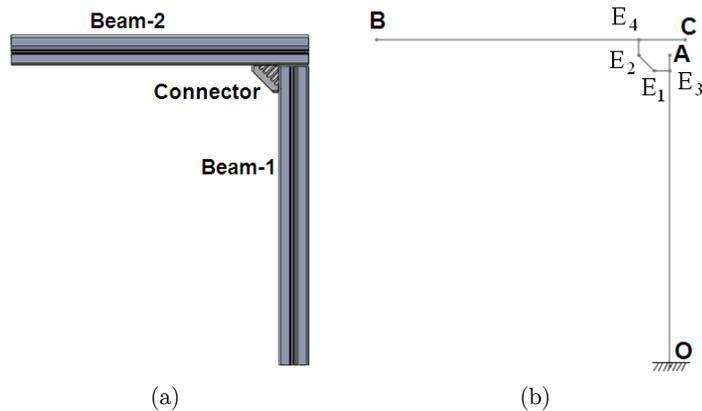

Figure 3: (a) Solid model, (b) Line model

Beam-1 and Beam-2 are created by the extrusions of corresponding cross-sections along the lines OA, and BC respectively. The extension beams are assumed on the lines E_1E_3 and E_2E_4. An equivalent beam for the connector is assumed on the line E_1E_2. E_1 and E_2 are at the mid-points of mating faces of the connector. The cross section of an extension beam is assumed to be the same as the adjacent beam. For example, E_1E_3 extension beam is assumed to have the same cross section as OA-beam. A negligible value (1 kg/m^3) is assigned to the densities (ρ) of extension beams.

The properties of the cross sections of the equivalent beams of connectors are assigned by analyzing L-frames as shown in Figure 3. Finite element analysis results are obtained by using solid finite elements and beam finite elements. The structure is fixed at O. Natural frequencies for the first two modes and the end point deflections at B under static loads are compared. The cross section properties of the connector are found by iteration so that the solid finite element results match with the beam finite element results. The value of ρ for an equivalent connector beam is assigned so that the equivalent connector beam has the same mass as the real connector.

In the FE model, the nodes of the elements on meshed beam lines of profiles are not directly merged with meshed beam lines of connectors. A finite element size L_e is defined. ANSYS generates beam finite elements with a size of L_e. L_e is chosen so that the divisions of all the lengths of the beams to L_e give integers without remainders. The nodes are merged by the command "*nummrg,node*" in ANSYS. Thus, the connection between the meshed beam lines of profiles and meshed beam lines of connectors are established in the model.

The lines for the beam FE model of Frame-TS-1A are shown in Figure 4. The location of a point (Point-A) on the line model of a system is defined by $R_A = [x_A, y_A, z_A]$, where x_A, y_A, and z_A are global Cartesian coordinates. O is the global origin. The locations of the points which are used for the results below are given in the figure. These points are used as excitation or sensor points below.
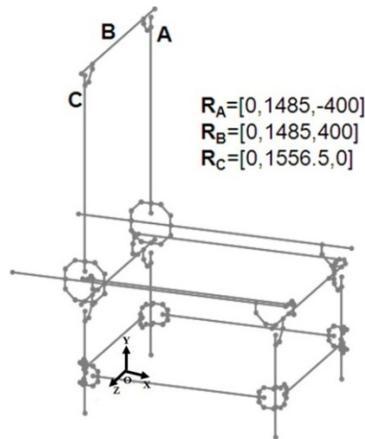

$R_A=[0,1485,-400]$
$R_B=[0,1485,400]$
$R_C=[0,1556.5,0]$

Figure 4: Line model of Frame-TS-1A

BEAM44 elements are used in ANSYS for beams. BEAM44 is a uniaxial element with tension, compression, torsion, and bending capabilities. The element has 6 degrees of freedom at each node: translations in the nodal x, y, and z directions and rotations about the nodal x, y, and z-axes. This element allows a different unsymmetrical geometry at each end and permits the end nodes to be offset from the centroidal axis of the beam. The details of the element are given in theory reference of ANSYS (ANSYS (2009)). Let a beam element has the nodes at the points I and J. The cross section of an element at I is shown in Figure 5, schematically.
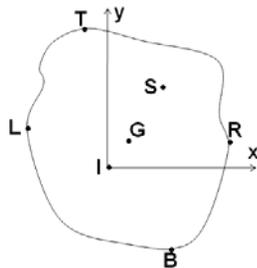

Figure 5: Cross section of beam element at Node-I

x and y are the nodal coordinates in the figure. G is the area center of gravity. S is the shear center. The geometrical properties of the cross section for the FE analysis is given by $p_s = [A, I_{Gx}, I_{Gy}, I_{Gz}, S_{dx}, S_{dy}, y_T, y_B, x_L, x_R]$ and $q_G=[x_G, y_G]$. Here, A is the area (cm^2); I_{Gx} is the area moment of inertia with respect to (w.r.t.) the axis in the x direction passing through G. I_{Gy} is the area moment of inertia w.r.t. the axis in the y direction passing through G. I_{Gz} is the moment of inertia

w.r.t. the axis in the z direction passing through G. I_{Gz} equals to the polar moment of inertia if $I_{Gz}=I_{Gx}+I_{Gy}$. $I_{Gz}=I_{Gt}$, if I_{Gz} equals to the torsional moment of inertia. The units of area moment of inertias are taken as cm^4 unless otherwise is stated. S_{dx} and S_{dy} are the shear deflection constants. T, B, L, R are the points on the fibers at extreme distances from G. x_G and y_G are the nodal coordinates of G. $q_G= [0, 0]$ if there is no offset between the nodal origin and the area center of gravity of the cross section. It is assumed that there is no offset unless it is stated. The geometrical properties of the beams are given in Table 4. The cross-sectional properties of beams are found by importing cross-section files to ANSYS.

Beam	p_s
s90x90	[38.9,301.9,301.9,152.9,3.25,3.25,45,45,45,45]
s90x90L	[23.56,211.1,211.1,105.4,5.27,5.27,45,45,45,45]
s45x45L	[5.7,11,11,1.7,4.24,4.22,22.5,22.5,22.5,22.5]
s90x45L	[11.29,23.6,81.9,12.9,4.47,3.25,3.25,22.5,22.5,45,45]
s30x30	[3.2,2.8,2.8,.3,3.34,3.34,3.34,15,15,15,15]
cn90	[3,5.85,7.5,24.21,2.49,1.89,43,43,43,43]
cn45	[1.23,0.87,1.15,1.42,2.12,2.12,11,11,11,11]
cn30	[3.2,2.8,2.8,.3,3.34,3.34,3.34,15,15,15,15]

Table 4: Geometrical properties of beams

4   MODELING SOFTWARE

A computer program to create SolidWorks and ANSYS models of aluminum profile framing (APF) systems has been developed in VisualBASIC. The users can create a database file for APF systems. The database contains the following information for FE analysis of frames: the information about the beams and connectors as listed in Table 3; the information about the boundary conditions, the meshing size; the geometrical properties of cross sections, and the material properties. User interface of the developed computer program is shown in Figure 6. The list of the operations is given in Table 5. The execution of the operations is activated by clicking the corresponding command options. The operations are achieved by using the input database and Application Programming Interface (API) capabilities of SolidWorks.
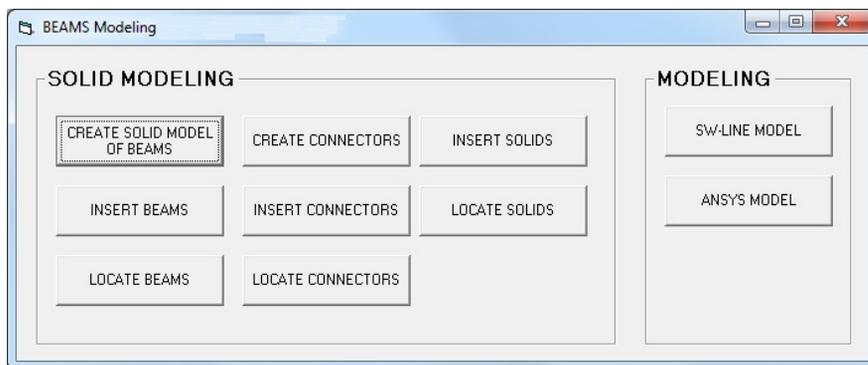

Figure 6: User interface of developed computer program.

Command label	Operation
Create solid models of beams	Imports cross-section files, extrudes along beam lines, and saves to files named by labels, in SolidWorks.
Insert beams	Inserts beams to assembly file in SolidWorks.
Locate beams	Locates beams in assembly.
Create connectors	Copies connector files to files named by labels, in SolidWorks.
Insert connectors	Inserts connectors to assembly file.
Locate connectors	Locates connectors in assembly.
SW-line model	Displays lines in SolidWorks.
ANSYS model	Creates ANSYS model.

Table 5: List of operations of modeling software

5 MEASUREMENT SYSTEM

The measurement system for obtaining experimental results is shown in Figure 7. The wireless vibration sensor is a MicroStrain G-Link tri-axial accelerometer (Accelerometer range: $\pm$ 10 g, 47 g, 58 mm x 43 mm x 26 mm). The wireless base station is MicroStrain Gateway WSDA-Base-104. The data received by the base station is transmitted to the computer through Universal Serial Bus (USB) and recorded by using Node Commander Software. The sampling rate is 2048 Hz. The frame is excited by a hammer impact. The FFTs (Fast Fourier Transforms) of the recorded signals in the x, y, and z directions are taken in MatLAB. The frequencies where the peaks appear are determined for the natural frequencies.

Figure 7: Photos of measurement system.

6 RESULTS AND DISCUSSIONS

6.1 L-Frame (LF-45)

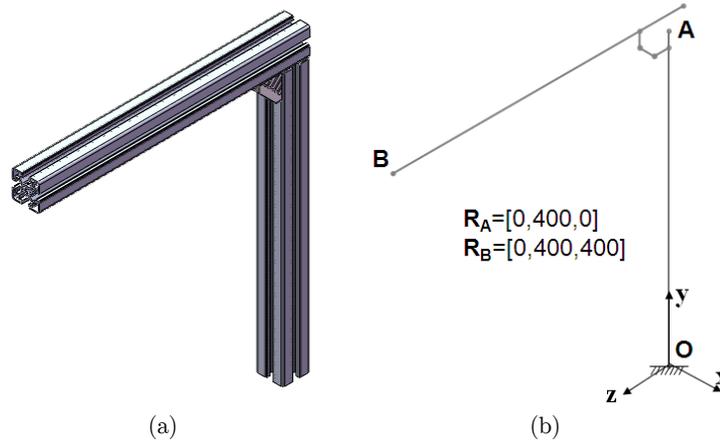A simple frame (LF-45) as shown in Figure 8 is considered. The database for the LF-45 is given in Table 6.

(a)   (b)

Figure 8: L-frame (LF-45) (a) Solid model for simulations (b) line model.

Label	File name	L_b	q_L
b01	s45x45	450	[0,0,0,-90,0,0]
b02	s45x45	450	[0,472.5,-22.5,-0,0,0]
c01	cn45	-	[0,450,22.5,90,0,0]

Table 6: Database for L-frame (LF-45)

The properties of the computers used to obtain FE results are given in Table 7. The solution time (s) for Type-1 computer is t_1, the solution time (s) for Type-2 computer is t_2, the number of nodes for FE analysis is n_d, and these values are given by $s_p=[t_1,t_2,n_d]$.

Computer	Properties
Type-1	WORKSTATION Intel Xeon X5687 3.6 GHz, 24 GB RAM, 64 Bit Win7 Operating System
Type-2	AMD PHENOM II X4 955- 3.2 GHz, 8GB RAM, 64 Bit Win7 Operating System

Table 7: Properties of computers

The modal analysis results are given in Table 8. Mode shapes of LF-45 which are obtained in ANSYS with solid finite elements are depicted in Figure 9. f_{ty}, f_{bx}, f_{bz} are natural frequencies corresponding to the mode shapes where the frame mainly makes torsional vibration about the y-axis (Mode-ty), bending vibration about the x-axis (Mode-bx), and bending vibration about the z-axis (Mode-bz), respectively. The information about the geometrical parameters for a measurement is given by $p_g = [z, A, B]$ as an example. z is the direction of the excitation and the signal component, A is the excitation point, and B is the sensor point. The excitation is an impact. The FFT's of the signal components and acceleration signal for the experimental results in Table 8 are given in Figure 10.

	Simulation		
	f_{ty} (Hz)	f_{bx} (Hz)	f_{bz} (Hz)
Solid FE $s_p=[38,52, 103399]$	22.53	50.54	113.27
Beam FE ($I_{Gz}=I_{Gx}+I_{Gy}$) $s_p=[<1,<1,3909]$	50.08[a]	54.51	128.65
Beam FE ($I_{Gz}=J_{Gt}$) $s_p=[<1,<1,3909]$	21.35	54.51	111.28
	Experiment		
	21.01 $p_g=[x, B, B]$	45.03 $p_g=[z, A, B]$	84.05 $p_g=[x, A, B]$

[a] Mode shape is different than torsional vibration about the y-axis
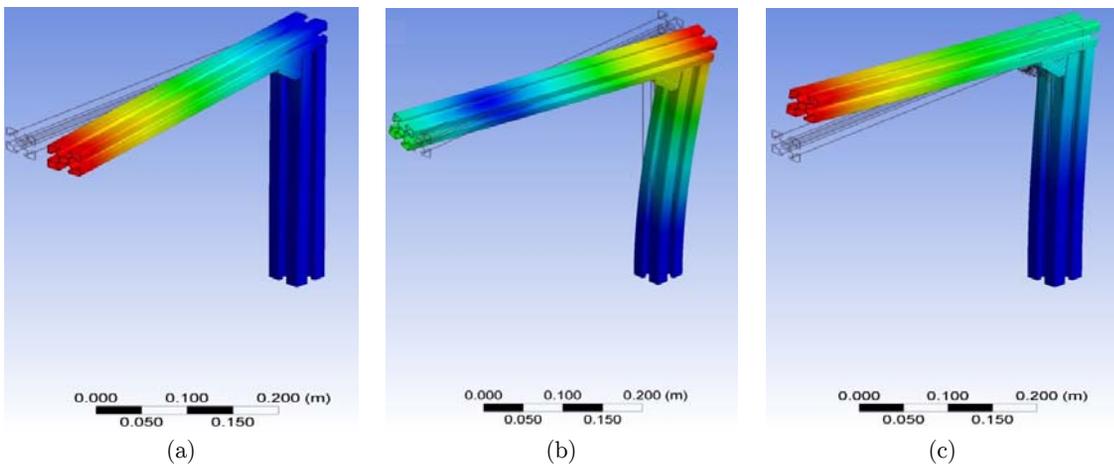
Table 8: Natural frequencies for LF-45

Figure 9: Mode shapes of LF-45 with solid finite elements for LF-45, (a) Mode-ty, (b) Mode-bx, (c) Mode-bz.
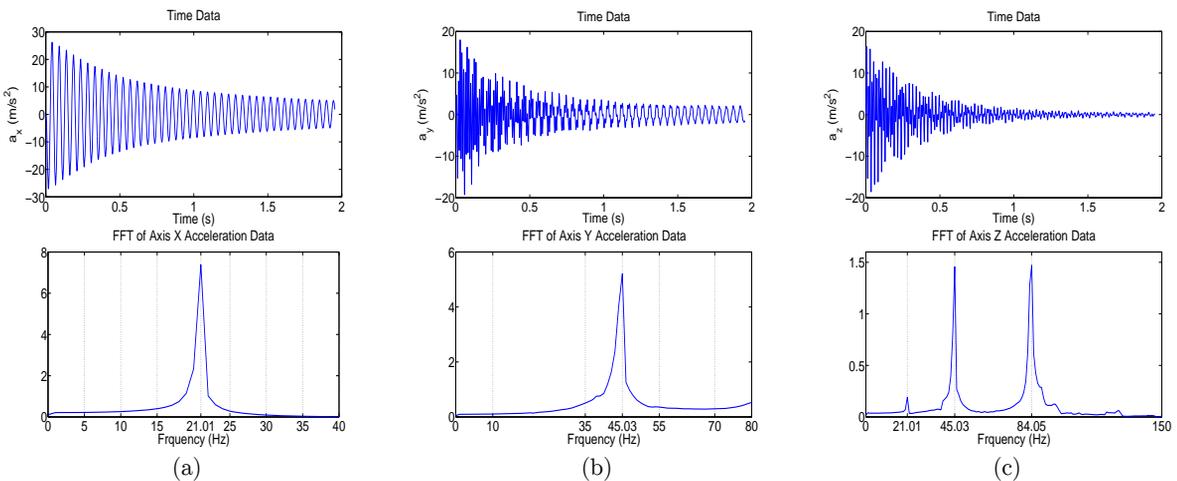

Figure 10: FFT's of signal components and acceleration signal for experimental results in
Table 8 for (a) Mode-ty, (b) Mode-bx, (c) Mode-bz

The excitation point and direction and the sensor axis (component) are chosen so that mainly the mode of interest is excited. The maximum values of the amplitudes of FFT's give the experimental natural frequencies. It is observed from Table 8 that the simulation result for Mode-ty is highly different than the experimental result if the polar moment of inertia were used. The use of torsional moment of inertia is important to obtain matching simulation and experimental results. The experimental values are smaller than the simulation results.

6.1 Frames (TS-1)

The results are given for Frame TS-1A, Frame TS-1B, and Frame TS-1C in this section. The database for Frame TS-1A shown in Figure 1 is given in Table 3. Frame TS-1B is obtained by reinforcing Frame TS-1A. Frame TS-1C is obtained by reinforcing TS-1B. Added components are given in Tables 9 and 10. Reinforcing is carried out by considering the mode shapes. The photos of Frame TS-1B and Frame TS-1C are shown in Figure 11.
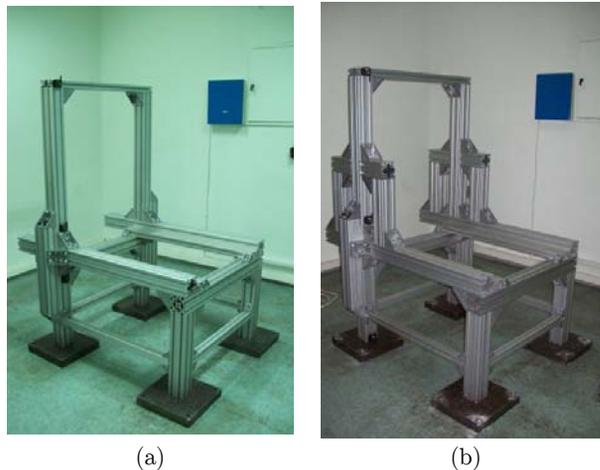

(a)   (b)

Figure 11: Photos of (a) Frame TS-1B, and (b) Frame TS-1C

Label	File name	L_b	q_L
bt01	s90x90L	L	[0,h,490,-90,0,0]
bt02	s90x90L	L	[0,h,-490,-90,0,0]
ct01	cn90	-	[0,h,445,90,0,0]
ct02	cn90	-	[0,h+L,445,0,0,0]
ct03	cn90	-	[0,h,-445,180,0,0]
ct04	cn90	-	[0,h+L,-445,-90,0,0]
ct05	cn90	-	[45,599,445,0,0,-90]
ct06	cn90	-	[-45,599,445,0,0,90]
ct07	cn90	-	[45,599,-445,-90,0,-90]
ct08	cn90	-	[-45,599,-445,-90,0,90]

[a]h is changed. L=530, h=240 unless otherwise stated

Table 9: Added component to TS-1A for TS-1B

Label	File name	L_b	q_L
bt03	s90x90L	355	[-188.5,644,400,-90,0,0]
bt04	s90x90L	188.5	[-233.5,1044,400,0,90,0]
bt05	s90x90L	355	[-188.5,644,-400,-90,0,0]
bt06	s90x90L	188.5	[-233.5,1044,-400,0,90,0]
bt07	s90x90L	355	[188.5,644,400,-90,0,0]
bt08	s90x90L	188.5	[233.5,1044,400,0,-90,0]
bt09	s90x90L	355	[188.5,644,-400,-90,0,0]
bt10	s90x90L	188.5	[233.5,1044,-400,0,-90,0]
ct09	cn90	-	[45,1089,400,0,90,0]
ct10	cn90	-	[143.5,999,400,0,-90,90]
ct11	cn90	-	[233.5,644,400,0,90,0]
ct12	cn90	-	[45,1089,-400,0,90,0]
ct13	cn90	-	[143.5,999,-400,0,-90,90]
ct14	cn90	-	[233.5,644,-400,0,90,0]

Table 10: Added component to TS-1B for TS-1C.

The results are given in Tables 11, 12, and 13 for Frame TS-1A, TS-1B, and TS-1C, respectively. The mode shapes obtained from simulation of TS-1 B are depicted in Figure 12. See Figure 4 for the locations of the excitation and the sensor points.
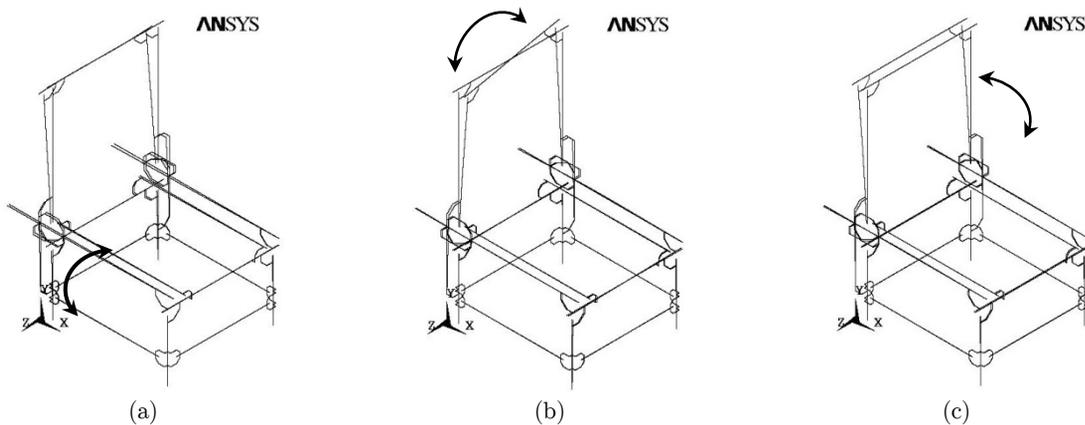

(a)   (b)   (c)

Figure 12: Mode shapes of Frame TS-1B, (a) Mode-bx, (b) Mode-ty, (c) Mode-bz

The simulation results given in Table 11 show that Mode-bx, Mode-bz, and Mode-ty have natural frequencies of 31.52, 40.34, and 58.06 Hz. These frequencies increase by 12.20, 2.54, and 3.16 Hz, respectively, for TS-1B as observed in Table 12. These frequencies increase by 5.31, 10.28, and 3.19 Hz, respectively, for TS-1C as observed in Table 13.

		f_{bx} (Mode-bx)	f_{bz} (Mode-bz)	f_{ty} (Mode-ty)
Simulation	Beam FE ($I_{Gz}=J_{Gt}$) $s_p=[15,19,149317]$	31.52	40.34	58.06
Experiment		30.74 $p_g=[z, A, C]$	39.42 $p_g=[x, B, C]$	56.35 $p_g=[x, A, C]$

Table 11: Natural frequencies for Frame TS-1A

		f_{bx} (Mode-bx)	f_{bz} (Mode-bz)	f_{ty} (Mode-ty)
Simulation	Beam FE($I_{Gz}=J_{Gt}$) $s_p=[16,23,166911]$	43.72	42.88	61.22
Experiment		38.91 $p_g=[z, A, C]$	41.98 $p_g=[x, B, C]$	61.46 $p_g=[x, A, C]$

Table 12: Natural frequencies for Frame TS-1B

		f_{bx} (Mode-bx)	f_{bz} (Mode-bz)	f_{ty} (Mode-ty)
Simulation	Beam FE($I_{Gz}=J_{Gt}$) $s_p=[19,27,199059]$	36.83	50.62	61.25
Experiment		33.29 $p_g=[z, A, C]$	43.53 $p_g=[x, B, C]$	58.89 $p_g=[x, A, C]$

Table 13: Natural frequencies for Frame TS-1C

The experimental results given in Table 11 show that Mode-bx, Mode-bz, and Mode-ty have natural frequencies of 30.74, 39.42, and 56.35 Hz. These frequencies increase by 8.17, 2.56, and 5.11 Hz, respectively, for TS-1B as observed in Table 12. These frequencies increase by 2.55, 4.11, and 2.54 Hz, respectively, for TS-1C as observed in Table 13.

The simulation and experimental results show similar trend for increasing natural frequencies with reinforcement. Reinforcing in TS-1B is more effective to increase the natural frequencies. Natural frequencies increase as stiffness/mass ratio effect of reinforcing increase.

7   CONCLUSIONS

In this paper, the finite element analysis of frames with aluminum profiles was carried out. It was observed that the analysis by solid finite elements was not possible because the cross sections of aluminum profiles had complicated shapes. Then, as an alternative approach, beam finite elements were used. A database was created for a frame. The database contained the information about the beams and connectors. A VisualBASIC program was developed to construct the model of the frame in the preprocessor of ANSYS automatically by using the database. The program also created solid model or line model in SolidWorks using the same database automatically. SolidWorks was used to evaluate the model visually, and the solver and postprocessor of ANSYS were used to obtain analysis results. BEAM44 element in ANSYS was used.

Assumptions were made to model connectors with beams. Simulation and experimental results were given for different frames. The results show that the approach developed in the present article can be used to design frames with aluminum profiles, which are commonly used in many engineering applications.

Acknowledgements

References

Akdağ, M., Karagülle, H. and Malgaca, L. (2012). An integrated approach for simulation of mechatronic systems applied to a hexapod robot. Mathematics and Computers in Simulation, 82:818-835

Bosch Rexroth AG.(2013.) Basic Mechanical Elements, 3 842 540 392.

Fadden, M. and McCormick, J.(2014). Finite element model of the cyclic bending behavior of hollow structural sections. Journal of Constructional Steel Research. 94: 64–75.

Fiorino, L., Macillo, V. and Mazzolani, FM .(2014) Mechanical behaviour of bolt-channel joining technology for aluminium structures. Construction and Building Materials 73: 76–88.

Fiorino, L., Macillo, V., Mazzolani, FM.(2013). Screwed joint for aluminium extrusions: experimental and numerical investigation. In:12th INALCO conference, Montreal 21–22 October 159–169.

Güler, S.(2013) Finite element analysis of a vertical machining center with aluminum profile framing. PhD Thesis, Dokuz Eylül University, İzmir, Turkey.

Hana, LH.,Wanga, WD., Zhao, XL.(2008). Behaviour of steel beam to concrete-filled SHS column frames: Finite element model and verifications. Engineering Structures 30, (6):1647–1658.

http://www1.ansys.com/customer/content/documentation/121/ans_thry.pdfs (2009) Accessed 10 March 2010

Kwon, HC., Im, YT., Ji, DC. and Rhee, M.H.(2001). The bending of an aluminium structural frame with a rubber pad. Journal of Materials Processing Technolog.113(1–3): 786–791.

Macillo, V., Fiorino, L. and Mazzolani, FM.(2013). Structural behavior of aluminium bolt channel joint: calibration of numerical models on testing results, In: 12th INALCO conference, 148-158, Montreal 21–22 October (2013).

Mazzolani FM. (2006). Structural applications of aluminium in civil engineering. Structural Engineering International, International Association for Bridge and Structural Engineering. 16:280-285.

Mazzolani, FM.(1995). Aluminium Alloy Structures. 2nd ed. London: E & FN SPON.

Microsoft. Help for Visual Basic 6 Users. https://msdn.microsoft.com/en-us/library/kehz1dz1(v=vs.90).aspx. (2012) Accessed 27 April 2012.

Rao, SS.(2011). Mechanical Vibrations. 3rd ed. Upper Saddle River: Prentice Hall.

Sangle, KK., Bajoria, KM. and Talicotti, RS.(2012) Elastic stability analysis of cold-formed pallet rack structures with semi-rigid connections. Journal of Constructional Steel Research. 71, 245–262.

Solidworks Web Help, Solidworks Corporation, http://help.solidworks.com (2012). Accessed 27 April 2012

Theory Reference for the Mechanical APDL and Mechanical Applications, ANSYS Release12.1:

Wu, JJ.(2004). Finite element modelling and experimental modal testing of a three dimensional framework. International Journal of Mechanical Sciences. 46: 1245–1266.

Wu, JJ.(2006). Finite element analysis and vibration testing of a three-dimensional crane structure. Measurement. 39 (8), 740–749.

Wu, JJ.(2008). Transverse and longitudinal vibrations of a frame structure due to a moving trolley and the hoisted object using moving finite element. International Journal of Mechanical Sciences. 50 (4): 613–625.

Zaeh, M. and Siedl, D.(2007) A new method for simulation of machining performance by integrating finite element and multi-body simulation for machine tools. Annals of the CIRP. 56: 383-386.

Zaeh, MF. and Oertli, T.(2004). Finite element modelling of ball screw feed drive systems. CIRP Annals - Manufacturing Technology. 53, 289-292.